Publications of the Laboratory of Data Analysis
Data-analyysin laboratorion julkaisuja No. 4

Determination of Fibre Orientation Distribution from Images of Fibre Networks

Markku Kellomäki, Salme Kärkkäinen, Antti Penttinen and Timo Lappalainen

Center for Computational and Mathematical Modeling
University of Jyväskylä
2003

Publications of the Laboratory of Data Analysis
Data-analyysin laboratorion julkaisuja

Distribution:
Laboratory of Data Analysis
Center for Computational and Mathematical Modeling
University of Jyväskylä
P.O.Box 20
FIN-53851 Jyväskylä
Finland

Electronic publications: http://erin.mit.jyu.fi/datalab/publications

Publications of the Laboratory of Data Analysis
Data-analyysin laboratorion julkaisuja
Jyväskylä 2003 No. 4

Determination of Fibre Orientation Distribution from Images of Fibre Networks

Markku Kellomäki, Salme Kärkkäinen, Antti Penttinen and Timo Lappalainen

Center for Computational and Mathematical Modeling
University of Jyväskylä
2003

Laboratory of Data Analysis
University of Jyväskylä
Jyväskylä 2003
ISBN 951-39-1526-3
ISSN 1458-7254

Contents

Abstract

We recall two categories of algorithms for estimating fibre orientation distribution from an image of a spatial fibre system. In the first algorithm, the estimate is a magnitude-weighted distribution from angles perpendicular to the directions of the gradients in the image. The second algorithm is based on the scaled variogram of grey values scanned along a sampling line and its relation to the fibre orientation distribution. Using lines in several directions and assuming a parametric model for the orientation distribution, the orientation parameters are estimated numerically from a least-squares type procedure. Two versions of variogram-based methods are used in this work. We compare the potential of these three methods by simulated images of fibrous layers and their thresholded versions. All the methods were found to reproduce the original distribution with a good accuracy in the case of greyscale images where grammage, anisotropy and orientation angle are within the typical ranges of paper parameters. On the contrary, the variogram-based methods seem to handle the estimation of anisotropy in binary images more efficiently.

1 Introduction

The practical motivation of this work arises from paper technology. Uneven fibre orientation distribution causes anisotropy to strength and stiffness of paper, and may induce curling of paper in printing machines. A recent trend in the laboratoric fibre orientation analysis is digital imaging and image analysis. In this work, three image-based methods for the determination of fibre orientation have been compared by computer simulation. This paper is an extension of the conference presentation by Kellomäki et al. (2002). In this work we present in more detail the simulation design and the obtained results, and conclude in the view of paper industry.

In a laboratory, fibre orientation distribution has conventionally been estimated indirectly by measuring the rates of ultrasound through paper along lines at various polar angles with respect to the machine direction, cf. e.g. Hutten (1994). The importance of fibre orientation as one of the paper making parameters has emerged by Loewen (1997), and Erkkilä et al. (1998) where the layered fibre orientation from images of paper layers extracted by sheet splitting has been studied. Further, sheet splitting, cf. Thorpe (1999), and confocal microscopy, cf. Xu et al. (1999), along with Hough transform image analysis have been applied. In Johansson (2002), the image-based orientation analysis of fibres on the paper surface is founded on the covariance function of a shot-noise model.

The availability of on-line sensors for fibre orientation have been promoted by Piispanen (2000) and Chapman et al. (2001). The on-line sensor is based on the combination of the reflection of laser light, and the polarization between the source and the sensor of laser light. It measures the orientation characteristics on both sides of paper lines such that the effect of the filling material is minimized. This is an advantage compared to the ultrasound tester.

In this work we focus on the comparison of three image-based methods for the estimation of fibre orientation in paper layers, cf. Erkkilä et al. (1998), Kärkkäinen et al. (2001), and Kärkkäinen and Jensen (2001). All these three methods essentially estimate the length of the boundary of fibres in a given direction interval (per area unit) but using different philosophy. In the method of Erkkilä et al. (1998), widely used in paper industry, the fibre boundaries are locally detected by gradient measurements. The empirical angular distribution is a distribution from local orientations perpendicular to the gradient field and weighted by the magnitudes of the gradients. The final estimate of fibre orientation distribution is obtained first presenting the empirical distribution in polar coordinates and then smoothing the empirical curve by fitting an ellipse to it. The two competitors suggested by Kärkkäinen et al. (2001), and Kärkkäinen and Jensen (2001), are based on the scaled variogram, which measures the variation of grey levels along a sampling line. The scaled variogram is shown to be in approximate relation with the number of intersected fibres by the line, and consequently, with the fibre orientation distribution, see Kärkkäinen et al. (2002) and also Jeulin (2000). The method in Kärkkäinen et al. (2001) is based on the proportional relation between the scaled variograms and the unobserved numbers of intersection points with respect to the sampling direction. It is theoretically

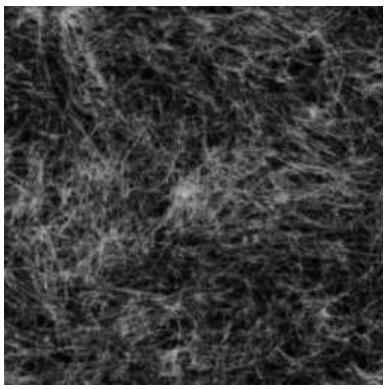

Figure 1: A greyscale image of 256×256 pixels with real size of 8.13 mm $\times$ 8.13 mm from a paper layer stripped by a tape technique.

addressed to digital greyscale (or binary) images of dead leaves models considered in Jeulin (1989, 1993). As an improvement, Kärkkäinen and Jensen (2001) suggest the use of a refined relationship between the scaled variograms and the intersection numbers. This relation is shown for digital binary images of Boolean fibres in Kärkkäinen et al. (2002). In the connection of both methods, a parametric model for orientation distribution is needed. Hence, the orientation parameters can be obtained numerically from a least-squares type procedure. The mutual advantages of these two different algorithms are not generally known.

In this study, the objective is to compare the accuracy and applicability of the methods in two types of paper industrial designs. The first design, the layered orientation analysis of paper, does not assume any special arrangement at the paper making stage. The paper sample is separated to several layers by an adhesive tape stripping technique, cf. Erkkilä et al. (1998) and Thorpe (1999). Each layer is scanned with an optical scanner. The image is a grammage map type image, where the grey level of a pixel is proportional to local grammage (or number) of fibres, cf. Figure 1. A question of industrial importance is to clarify the factors affecting the results in the estimation of the fibre orientation. The second design, the orientation analysis of coloured fibres on the paper surface, assumes that colouring of a percentage of fibres is a part of the production stage. This design can only be applied in experimental situations. Orientation analysis of dyed fibres on the paper surface can be based on the thresholded image, where solely stained fibres are shown, see Figure 2. A practical question is to approximate the optimal percentage of coloured fibres which results in a good precision of the estimates of orientation parameters. Due to practical reasons, low percentages in staining of paper fibres are advisable.

To objectively assess the potential of the three methods, we compare the methods by simulated images. Two types of models for fibre systems, shot-noise and binary (Boolean) models have been applied in the comparison, see e.g. Rice (1977) and Matheron (1975), respectively. The shot-noise model is a feasible model for the grammage map type images as well as for surface topography of fibre networks observed by high-resolution profilome-

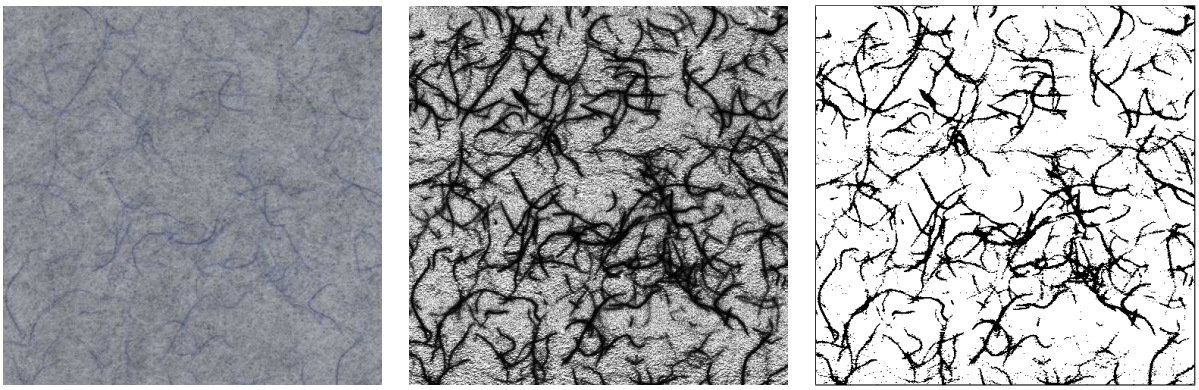

Figure 2: Illustration of the coloured fibres in an image of size 500×500 pixels with real size of 25.4 mm $\times$ 25.4 mm. Left: An image of the surface of a paper sample in which 0.1 percent of fibres are dyed. Middle: The image after contrasting. Right: The middle image after 20 % thresholding.

ter. The binary model is convenient in the case of thresholded images, e.g. recognition of dyed fibres or shadows of fibres in transmission imaging.

If the resolution of the grid in a digital image is low, according to results in Kärkkäinen et al. (2002), the accuracy of the variogram-based methods may be related to fibre parameters such as grammage (related to length fraction), anisotropy and direction of orientation angle. For the shot-noise and binary simulation models, we vary grammage, orientation angle and anisotropy of fibres in order to cover the range of parameters conventional in paper making. The effect of each parameter on the determination of anisotropy and orientation angle are studied using matched design, that is, the three methods are compared for the same simulated images. We pay attention to the bias and stability of the solution and evaluate the applicabilities of the orientation analysis methods for industrial use.

The content of this work is the following. Section 2 reviews the methods to be compared. In section 3 the binary and shot-noise models are introduced and the parameters to be varied are specified. Section 4 introduces the simulation results. Section 5 concludes the obtained results in the view of paper industry.

2 Methods for observing fibre orientation

2.1 Gradient-based method

In Erkkilä et al. (1998), the estimation method for orientation distribution of fibres in a greyscale image is based on gradient measurements. Gradients of grey values are locally perpendicular to the orientations of fibre boundaries. The estimate for the orientation distribution is a distribution of local orientation perpendicular to the gradient field and

weighted by local magnitude of the gradient.

To be precise, consider an observed image W as a grey-valued field $z(x)$. The gradient of $z(x)$ at $x = (x_1, x_2)$ is a vector

$$\nabla z(x) = \left(\frac{\partial z(x)}{\partial x_1}, \frac{\partial z(x)}{\partial x_2} \right). \tag{1}$$

Since the interest is in the orientation of the boundaries, let us consider the vector $\nabla^{\perp} z(x)$ perpendicular to $\nabla z(x)$. It is highest on the fibre boundary, lowest outside the fibre and inside it, and thus shows the direction of the fibre boundary. Let the local orientation angle of $\nabla^{\perp} z(x)$ be α. Then the orientation distribution can be defined, up to a scaling factor, as

$$f_W(\alpha) = \int_{W(\alpha)} |\nabla z(x)| dx. \tag{2}$$

Here, $W(\alpha)$ is the union of the small open sets in W, where $\nabla^{\perp} z(x)$ has direction α and magnitude $|\nabla^{\perp} z(x)| = |\nabla z(x)|$.

In practice, we consider a digital image of grey values $\{z(l,m)\}$ in pixels $\{(l,m) : \ l, m$ integers$\}$. The gradient $\nabla z(l,m)$ is approximated by the partial derivatives calculated using the convolution mask of size 5×5, cf. Erkkilä (1995). The estimated probability of the direction of a fibre belonging to a fixed interval $\triangle\alpha$ on $[0, 2\pi)$ is a division between the sum of magnitudes in the given interval and the sum of all magnitudes, formally

$$\hat{F}_W(\triangle\alpha) = \frac{\sum_{\alpha(l,m) \in \triangle\alpha} |\nabla z(l,m)|}{\sum_{(l,m) \in W} |\nabla z(l,m)|}, \tag{3}$$

where $\alpha(l,m)$ is the estimated angle perpendicular to the direction of the gradient in (l,m). As the length of $\triangle\alpha$, one degree is typically used. The final estimate of fibre orientation distribution is obtained first presenting the empirical distribution (3) in polar coordinates and then smoothing the empirical curve by fitting an ellipse to it.

2.2 Variogram-based methods

The two variogram-based methods for orientation analysis are based on the combination of stereology and image analysis, cf. Kärkkäinen et al. (2001), and Kärkkäinen and Jensen (2001).

The grey-valued random field $Z(x)$ of a fibre image is intersected by a sampling line L_β forming an angle β with respect to the x_1-axis, cf. Fig. 3. Under some regurality conditions, the variation in grey values on the sampling line carries information on the fibre orientation distribution, cf. Jeulin (2000) and Kärkkäinen et al. (2002). The variation is measured in terms of the scaled variogram of grey levels

$$V_L(d, \beta) = \frac{E|Z(x) - Z(y)|}{d}, \tag{4}$$

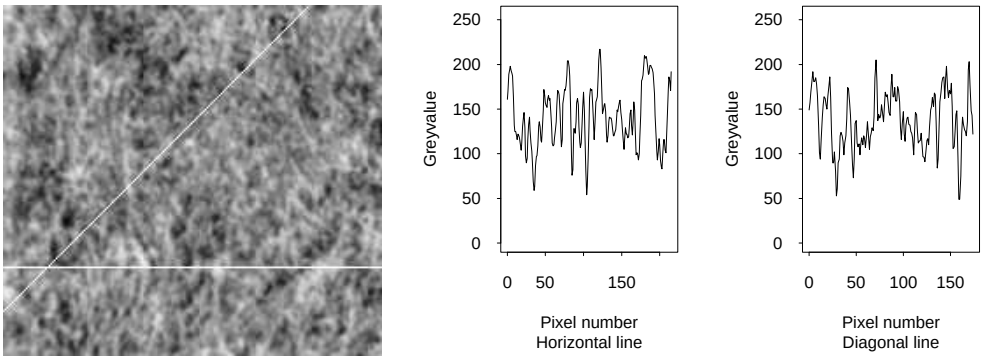

Figure 3: An image of paper fibres intersected by horizontal ($\beta = 0$) and diagonal ($\beta = \pi/4$) lines, and the pixel-valued functions obtained on the lines, cf. Kärkkäinen et al. (2001).

where $x, y \in \mathbb{R}^2$ are located on L_β at the distance $d = ||x-y||$, $Z(x)$ and $Z(y)$ are random grey values at x and at y, respectively, and $E|Z(x) - Z(y)|$ is the mean value of the absolute deviance. Kärkkäinen et al. (2001) employ the proportional model

$$V_L(d, \beta) \propto P_L(\beta) \tag{5}$$

with

$$P_L(\beta) = L_A \int_0^\pi |\sin(\alpha - \beta)| f(\alpha) d\alpha \,. \tag{6}$$

The quantity $P_L(\beta)$ is the mean number of intersection points between the fibres and a sampling line L_β, L_A the mean fibre length per area unit, and $f(\alpha)$ the target orientation distribution of fibres, cf. e.g. Mecke and Stoyan (1980). The equation (5) is shown for fibres in a greyscale (or binary) image generated by a dead leaves model, cf. Jeulin (2000) and Kärkkäinen et al. (2002). In Kärkkäinen and Jensen (2001), the use of the refined version

$$V_L(d, \beta) \propto \left(1 - \frac{d P_L(\beta)}{2}\right) P_L(\beta) \tag{7}$$

is suggested. The relation (7) is shown for binary images of Boolean fibres in Kärkkäinen et al. (2002).

In practice, the scaled variogram is calculated from the observed digital greyscale image $\{z(l, m) : \ l, m \text{ integers}\}$. We use the same digital lines $\bar{L}_{\beta_i}$ as in Kärkkäinen et al. (2001) and Kärkkäinen and Jensen (2001). The main directions are $\beta_1 = 0$, $\beta_3 = \pi/4 = 0.785$, $\beta_5 = \pi/2 = 1.571$, $\beta_7 = 3\pi/4 = 2.356$ with distances between adjacent pixels $d_1 = 1$, $d_3 = \sqrt{2}$, $d_5 = 1$, $d_7 = \sqrt{2}$, respectively. In the intermediate directions $\beta_2 = 0.464$, $\beta_4 = 1.107$, $\beta_6 = 2.034$, $\beta_8 = 2.678$, every second pair of adjacent pixels is located in the main direction β_{i-1} at the distance d_{i-1}, whereas every second pair is situated in the main direction β_{i+1} at the distance d_{i+1}. For β_8, however, the latter direction and

distance are $\beta_9 = \beta_0$ and $d_9 = d_0$, respectively. For the scaled variogram, we use the estimator

$$\hat{V}_L(\beta_i) = \frac{\sum_{(l,m),(l',m')\in \bar{L}_{\beta_i}} |z(l,m) - z(l',m')|}{\sum_{(l,m),(l',m')\in \bar{L}_{\beta_i}} ||(l,m) - (l',m')||}, \tag{8}$$

where the pixels (l,m) and (l',m') are adjacent. In each sampling direction, the image is scanned in the form of a bundle of parallel digital lines. Edge correction is not employed.

In order to determine the orientation parameters θ, let us define

$$F_i(\theta) = \int_0^\pi |\sin(\alpha - \beta_i)| f(\alpha;\theta) d\alpha \tag{9}$$

where $f(\alpha;\theta)$ is a parametric orientation distribution of fibres. It can be e.g. elliptic, cf. (14). In the case of the proportional model (5), from Kärkkäinen et al. (2001) we obtain the object of minimization procedure

$$\hat{\chi}(\theta) = \sum_{i=2}^{8} w_i \left(\hat{V}_L(\beta_i) - \hat{V}_L(\beta_1) \frac{G_i(\theta)}{G_1(\theta)} \right)^2 \tag{10}$$

with respect to θ. Here,

$$G_i(\theta) = \begin{cases} F_i(\theta), & \text{i=1,3,5,7} \\ \frac{d_{i-1}}{d_{i-1}+d_{i+1}} F_{i-1}(\theta) + \frac{d_{i+1}}{d_{i-1}+d_{i+1}} F_{i+1}(\theta), & \text{i=2,4,6,8} \end{cases}$$

and $w_i = L_i L_1/(L_i + L_1)$, where L_i is the total length of the digital line in the direction β_i for $i = 2, \ldots, 8$. According to Kärkkäinen and Jensen (2001), we will minimize in the refined case (7)

$$\hat{\chi}(\theta, L_A) = \sum_{i=2}^{8} w_i \left(\hat{V}_L(\beta_i) - \hat{V}_L(\beta_1) \frac{G_i(\theta, L_A)}{G_1(\theta, L_A)} \right)^2, \tag{11}$$

where

$$G_i(\theta, L_A) = F_i(\theta)[1 - d_i L_A F_i(\theta)/2] \tag{12}$$

holds for $i = 1, 3, 5, 7$ and

$$G_i(\theta, L_A) = \frac{d_{i-1}}{d_{i-1} + d_{i+1}} G_{i-1}(\theta, L_A) + \frac{d_{i+1}}{d_{i-1} + d_{i+1}} G_{i+1}(\theta, L_A) \tag{13}$$

for $i = 2, 4, 6, 8$.

3 Simulation design for fibrous structure of paper

In order to compare the methods, controlled samples generated by computer simulation were applied. The way how to construct the simulation model depends on which kind

of image is at our disposal. There are three choices concerning the parametric model. The first choice describes how the fibres are deposited. If the fibre orientation is to be determined from grammage map type images where the grey level of a pixel is proportional to local grammage (or number of fibres), an additive shot-noise model is the choice (Fig. 1). This model accumulates the local grammage. In the case of thresholded images, e.g. recognition of dyed fibres, the binary model simulates the fibre network best (Fig. 2). Secondly, we have to fix the size and shape of the fibres. This model consists essentially of the physical dimension of the fibres. The third choice is a model for the orientation distribution of fibres. After choosing the elements of the parametric model, the parameters and their ranges to be varied are specified. We use matched design. All three methods for orientation analysis are addressed to the same simulated images which improves the efficiency of simulation-based comparisons.

3.1 Simulation models

In the paper image, a random thick fibre Ξ on $\mathbb{R}^2$ is assumed to be a rectangle with fixed length l, fixed width $w << l$, and orientation distribution of the longer side of the fibre given by the elliptic density

$$f(\alpha;\tau,\kappa) = \frac{c}{\sqrt{1-\kappa^2\cos^2(\alpha-\tau)}}, \quad 0 \le \alpha < \pi, \tag{14}$$

cf. Kärkkäinen et al. (2001). Here c is the normalizing constant, $\tau \in [0,\pi)$ (the angle with the x_1-axis) is the preferred direction of fibres, and

$$\kappa = \sqrt{1-(b/a)^2} = \sqrt{1-(1-(1-e))^2} \in (0,1) \tag{15}$$

with a and b, the major and minor axes of the ellipse, describes deviation from the circular model ($\kappa = 0$). In paper industry, $1-e$ is conventionally used as a parameter for anisotropy. Furthermore, mean fibre coarseness δ is the mean mass per length unit of the paper fibre.

The thresholded image of dyed paper fibres can be approximated by a random binary field

$$Z(x) = 1_\Xi(x),\ x \in \mathbb{R}^2, \tag{16}$$

with

$$\Xi = \cup_{n=1}^{\infty}(x_n + \Xi_n). \tag{17}$$

Here, $\{x_n\}$ is a stationary random (Poisson) point process in $\mathbb{R}^2$ with the mean number of points per area unit λ (fibre density) and $\{\Xi_n\}$ is an i.i.d. sequence of rectangles and independent of $\{x_n\}$, cf. Stoyan et al. (1995). Ξ forms the Boolean model, cf. e.g. Matheron (1975). The global characteristics of Ξ are length fraction $L_A = \lambda l$, and mean grammage $G = L_A\delta$, which are total fibre length per area unit, and mean mass per area unit, respectively. Figure 6 illustrates binary images of Boolean models.

Figure 4: The enlargement of local grammage accumulation.

In a grammage map type image, the grey level of a pixel is proportional to local grammage (or number) of fibres. The fibre deposition, where grammage accumulates, can be modelled by a planar shot-noise model, cf. Rice (1977) and references therein. In the simplest form, it is constructed from the Boolean model Ξ as follows

$$Z_{shot}(x) = \sum_{\Xi_n \in \Xi} \delta \; 1_{\Xi_n}(x - x_n), \; x \in \mathbb{R}^2, \tag{18}$$

where $1_{\Xi_n}(x - x_n)$ indicates if Ξ_n hits the point x. In the positive case, the grammage is accumulated according to δ. Local accumulation of grammage is illustrated in Figure 4. The moments of the shot-noise model can be described directly using Campbells' theorem, see Schmidt (1985) and Stoyan et al. (1995).

3.2 Implementation

We demonstrate the discrete grammage map type images from paper using simulation of shot-noise models (18). We vary grammage, orientation angle and anisotropy of fibres covering the range of parameters conventional in the grammage map. The binary images (16) are resulted in thresholding the images of shot-noise models.

The paper fibres are simulated by identically and independently distributed rectangles with fixed length $l = 1$ mm, width $w = 0.02$ mm, mean fibre coarseness $\delta = 110$ μg/m, and random orientation. Orientation distribution in this study is uniform or elliptical (14) with parameters as follows. Orientation angle $\tau = \mathbf{90°}$ (MD), is used together with anisotropies

$$1 - e \in \{0.2, \; \mathbf{0.4}, \; \mathbf{0.5}, \; 0.6, \; 0.8\}$$

(industrially relevant values are written in bold). Further, orientation angles

$$\tau \in \{45°, \; 60°, \; \mathbf{75°}, \; \mathbf{105°}, \; 120°, \; 135°\}$$

are used with anisotropy value $1 - e = \mathbf{0.5}$. The fibre density is determined by λ, the mean number of points per area unit (per m^2), cf. Table 1. According to that, the mean grammage is varied

$$G \in \{0.3, \; 1.5, \; \mathbf{3.0}, \; \mathbf{6.0}, \; 12.0, \; 24.0\} \text{ g/m}^2.$$

Table 1: Mean numbers of points λ per m^2 and mean grammages $G = \lambda l \delta$ g/m^2 with fibre lenght $l = 1$ mm and mean fibre coarseness $\delta = 110$ μg/m used in simulation.

λ	G
2.732×10^{-6}	0.3
13.639×10^{-6}	1.5
27.278×10^{-6}	**3.0**
54.545×10^{-6}	**6.0**
109.090×10^{-6}	12.0
218.180×10^{-6}	24.0

Combining the six grammage values with the isotropic case, and the eleven combinations of the orientation angle and the anisotropy, we have totally 72 experimental points.

The resulted images are of size 7.68×7.68 mm^2($= 0.590$ cm^2) with 256×256 pixels, where the pixel side length is 0.03 mm. Then, for example, fibre length l and width w are 33.333 and 0.667 pixel sides, respectively. However, at the first stage of the deposition of fibres a grid with higher resolution has been used in order to decrease the effect of digitization, cf. Cresson (1988). This is illustrated in Figure 4. The boundary effect is eliminated using a suitable guard area.

The shot-noise model is generated by depositing individual fibres on the continuous plane and then projecting these fibres to a discrete matrix of given resolution, cf. Kellomäki et al. (2001). We simulate ten realizations of shot-noise images in each experimental point. The binary $\{0, 1\}$-valued image is obtained by thresholding the shot-noise image. Eventually, 1440 images are produced. In Figure 5, examples of shot-noise models are shown, and in Figure 6, the same images are transformed to binary images. Figure 7 illustrates the different orientation angles used only with anisotropy $1 - e = 0.5$. These orientation angles are applied with all grammage values and both simulation models. The images with weak anisotropy do not reveal clear difference between the directions of the orientation angle. The methods, however, exctract the orientation angle if there exists sufficiently information.

4 Results of comparison of different approaches

In the simulation of binary and shot-noise fibre models, we vary grammage, orientation angle, and anisotropy according to the design of Section 3. We study the effects of these factors on orientation angle and anisotropy determined by the gradient- and two variogram-based methods. Using the matched design, we calculate the mean anisotropy $(1-e)_{image}$ from the images (binary or shot-noise) and $(1-e)_{sim}$ directly from the simulated fibres. In the comparison, we use the ratio $(1 - e)_{image}/(1 - e)_{sim}$. Similarly in the comparison of orientation angles, we use the ratio τ_{image}/τ_{sim}, where τ_{image} is the mean

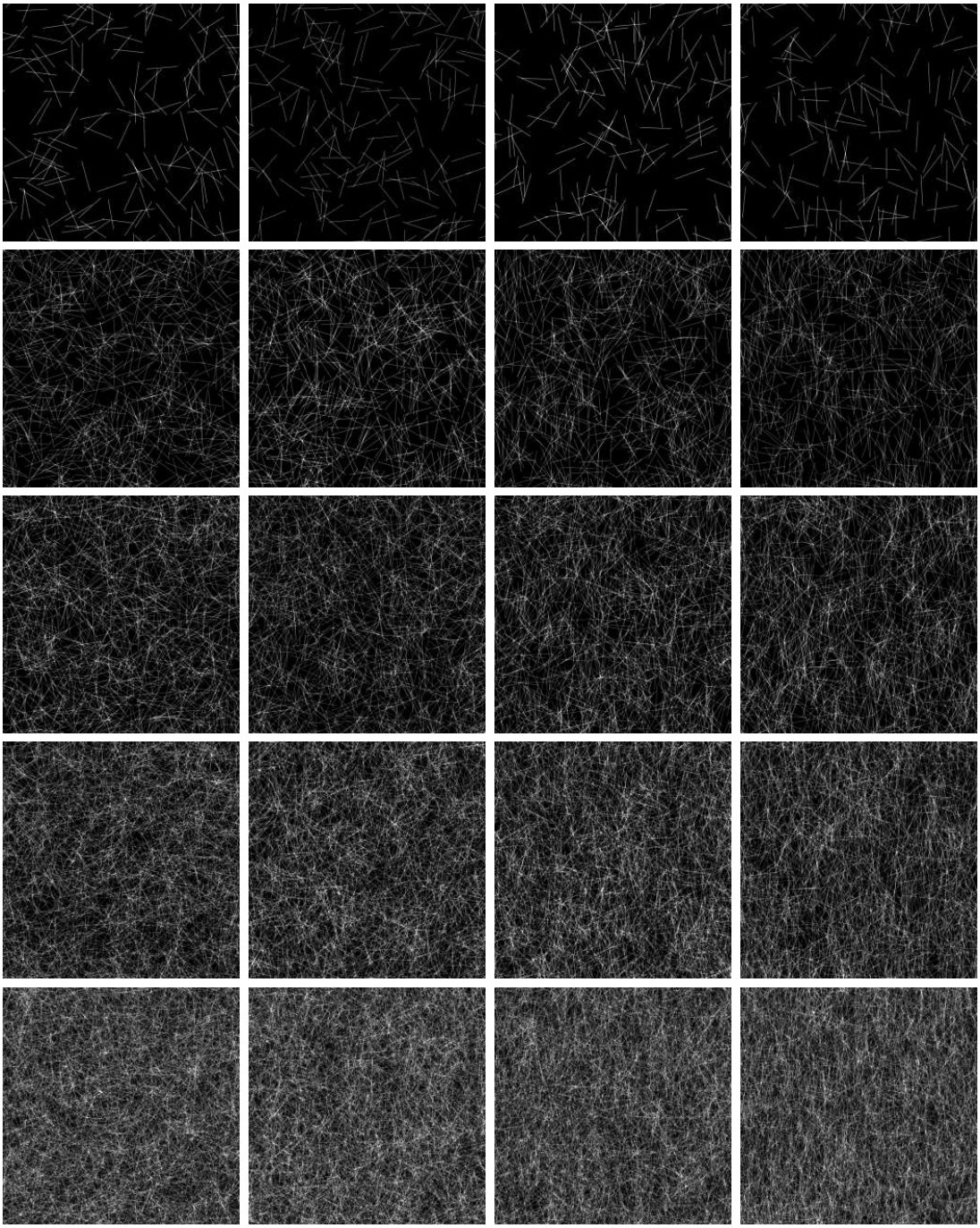

Figure 5: Illustration of shot-noise models: from left to right anisotropy values are $1 - e \in \{0,\ \mathbf{0.4},\ 0.6,\ 0.8\}$, and from top to down grammage values $G \in \{0.3,\ 1.5,\ \mathbf{3.0},\ \mathbf{6.0},\ 12.0\}$ g/m^2 with orientation angle **90°** upwards.

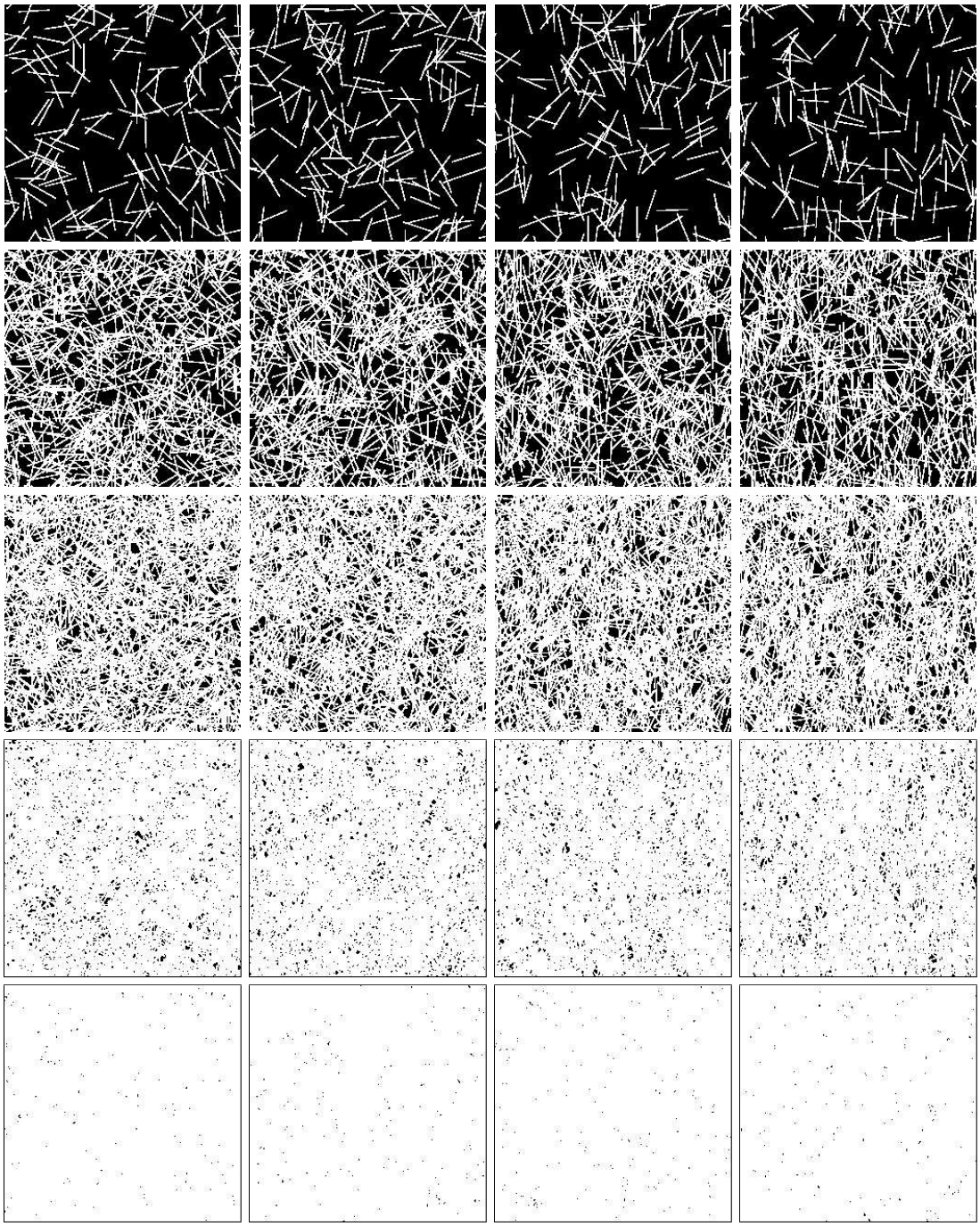

Figure 6: Illustration of binary models (thresholded from the images shown in Figure 5): from left to right anisotropy values are $1 - e \in \{0,\ \mathbf{0.4},\ 0.6,\ 0.8\}$, and from top to down grammage values $G \in \{0.3,\ 1.5,\ \mathbf{3.0},\ \mathbf{6.0},\ 12.0\}$ g/m^2 with orientation angle **90°** upwards.

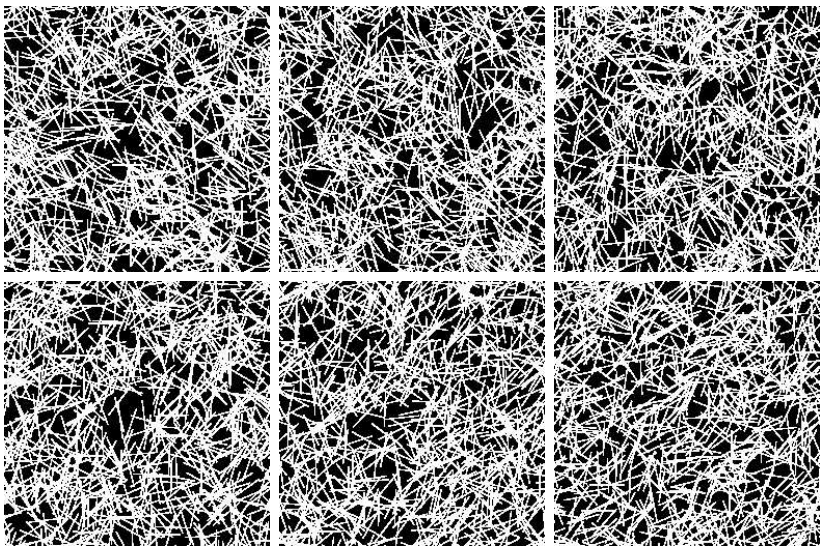

Figure 7: Illustration of orientation angles: from left to right in the upper row $\tau \in \{135°,\ 120°,\ \mathbf{105°}\}$, and in the lower row $\tau \in \{\mathbf{75°},\ 60°,\ 45°\}$. The anisotropy is $1 - e = \mathbf{0.5}$ and the grammage $G = 1.5$ g/m^2.

orientation angle calculated from the images and τ_{sim} from the fibres. Using the matched design and ratios, the effect of simulation on the estimation results has been eliminated. The ratio values near one indicate the unbiasedness of an image-based method. Due to the design in the determination of both anisotropy and orientation angle, we study firstly the effect of grammage and orientation angle (digitization) with fixed anisotropy $1 - e = 0.5$ and secondly the effect of grammage and anisotropy with fixed orientation angle 90°. In isotropic cases, $(1 - e)_{image}/(1 - e)_{sim}$ is, however, not defined, and the variogram-based methods addressed to elliptical densities suffer from the identication problem. Thus, the ratios in isotropic cases are not considered.

In the shot-noise case, when considering the determination of the anisotropy, the increase in grammage, the changes of orientation angle away from 90°, and the decrease in anisotropy worsen the result for all the methods according to Figure 8. In the determination of orientation angle, the decrease in anisotropy worsen the result for all methods. The changes in orientation angle seem to have the largest effect on the proportional method, cf. Figure 9. In the range of values of real paper, however, all the methods perform quite well. The gradient-based method is the most stable.

In the binary case, the image is almost saturated when $G = 12.0$ g/m^2, cf. Figure 6. Thus, it is sensible to consider results in more detail when $G = 6.0$ g/m^2 or less. The results of comparison are shown in Figures 10 and 11. In the determination of anisotropy, the gradient method is the most sensitive to the increase in grammage, whereas in the determination of orientation angle it performs well. The proportional method is sensitive to the increase in grammage if in addition the orientation angle is changed away from 90°; near 90°, however, the results for both parameters are good. The refined method is

applicable in a wider range than the proportional method, as was expected according to Kärkkäinen et al. (2002). In general, the refined method handles both the digitization and the increase in grammage most efficiently.

5 Conclusion

Three image-based methods for the determination of the fibre orientation distribution have been compared by computer simulation. Two types of models for fibre systems, shot-noise and binary (Boolean) random fields, have been applied in the comparison. The shot-noise models are feasible models for optical observations such as grammage map type images as well as for surface topography of fibre networks observed by high-resolution profilometer. Binary models are convenient for thresholded images of dyed fibres and shadows of fibres in transmission imaging.

Shot-noise and binary fibre models have been simulated by varying grammage, orientation angle and anisotropy of fibres. The effects of these factors on the determination of the orientation parameters are compared in the connection of three methods. In the binary case, the increase in grammage decreases the information to be used, since the image tends to saturate. In the shot-noise images, the situation is, however, better because as an additive process it does not suffer from saturation. The increase of anisotropy seems to affect positively, especially to variogram-based methods. Due to digitization, the determination of the orientation parameters performs best if the grid is close to the direction of the orientation angle as it, typically, is in the industrial images of paper. In general, the three methods perform quite well within the range of values of real paper when the shot-noise models are considered. The gradient method is the most stable. In the binary case, the variogram-based methods seem to perform better in the estimation of anisotropy. The refined method handles the increase in grammage and the digitization most efficiently.

In the orientation analysis of stained fibres through binary images, the percentages of stained fibres affect the results. For an efficient orientation analysis, we are able to give a suggestion for the highest grammage G (or intensity L_A) of fibres in binary images. In the determination of the anisotropy, the gradient method gives good results if the grammage is from $G = 0.3$ g/m^2 to $G = 1.5$ g/m^2, whereas in the determination of the angle, it works further until $G = 3.0$ g/m^2. When using the proportional method, the results are reasonable until $G = 6.0$ g/m^2 if the angle is near 90 °. The refined method is quite stable in the determination of both parameters until $G = 6.0$ g/m^2. From the practical point of view, the previous limits are, however, not applicable as such since they are not expressed in terms of the percentages of stained fibres in the suspension.

As a further task, similar comparisons of the three orientation analysis approaches could be done using the dead leaves model for greyscale images. In binary cases, the relation between the percentages of stained fibres and the grammage (or intensity L_A) limits is of interest in practice. Also, clarification of the lowest limit for grammage with a larger

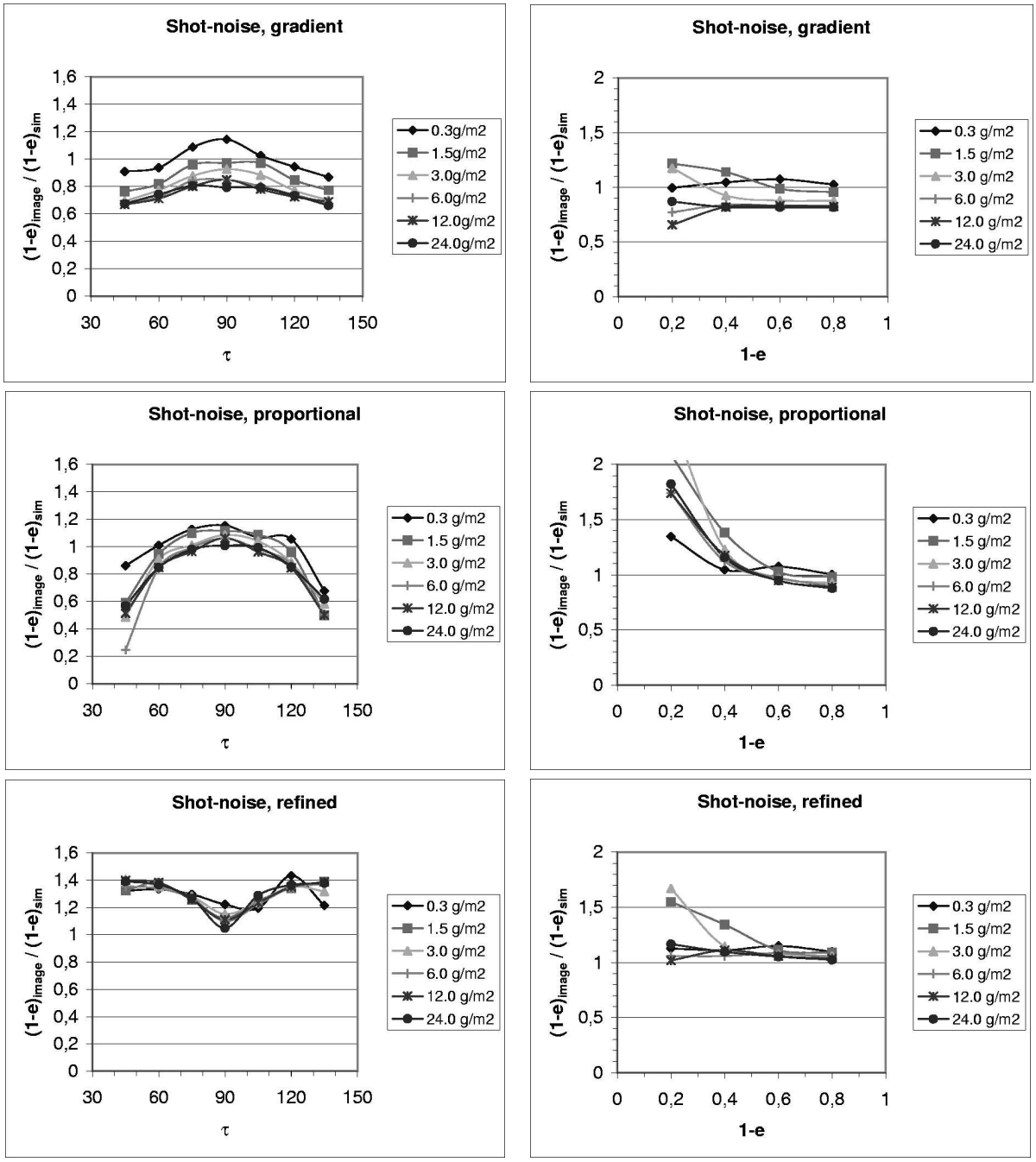

Figure 8: The determination of anisotropies in shot-noise cases with three methods. In all cases, the grammage G varies. On the left, the true anisotropy is fixed to $1 - e = 0.5$, whereas on the right the true angle is $\tau = 90°$.

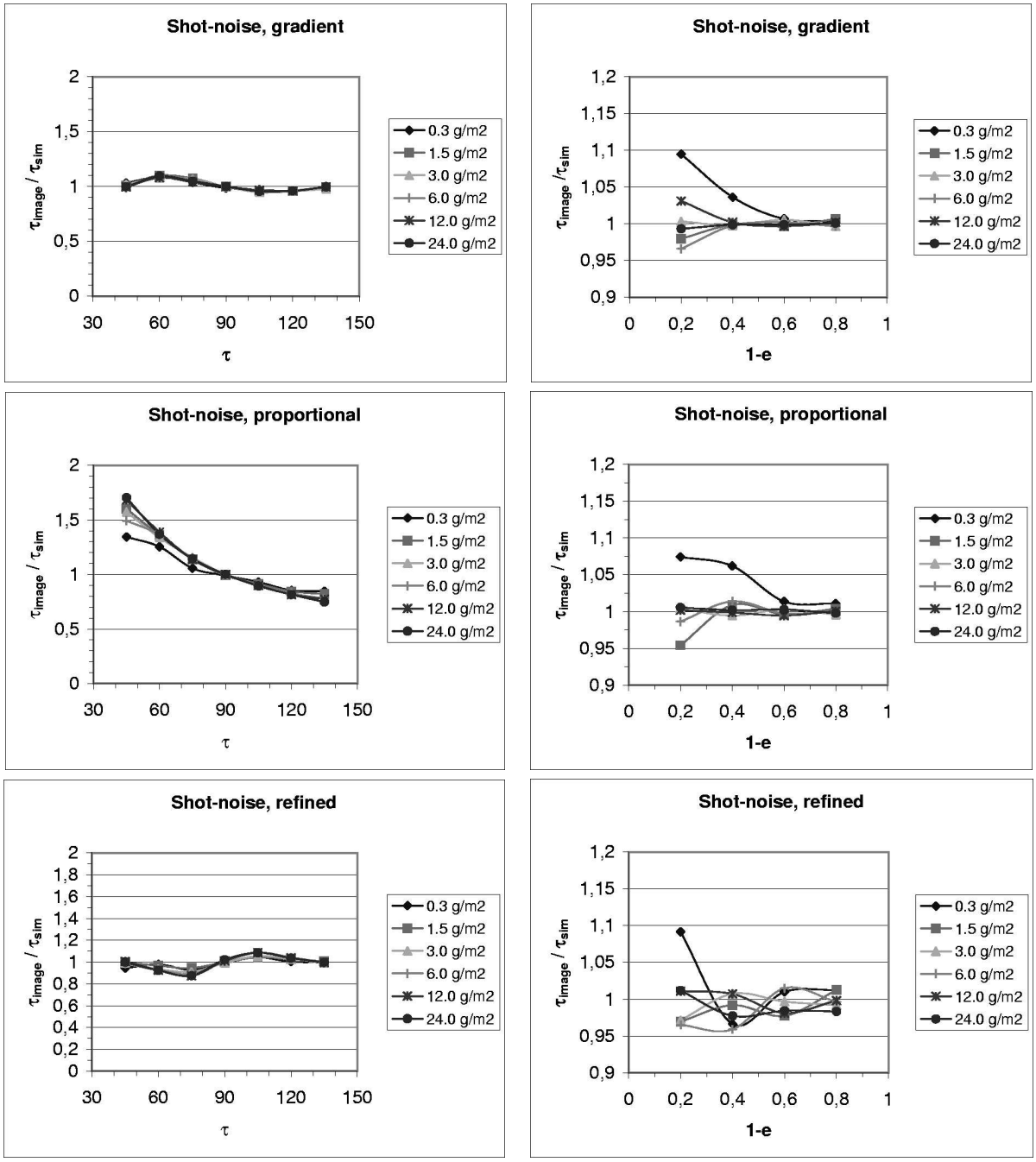

Figure 9: The determination of the angles τ in shot-noise cases with three methods. The grammage G varies in all cases. On the left, the true anisotropy is fixed to $1 - e = 0.5$, whereas on the right the true angle is $\tau = 90°$.

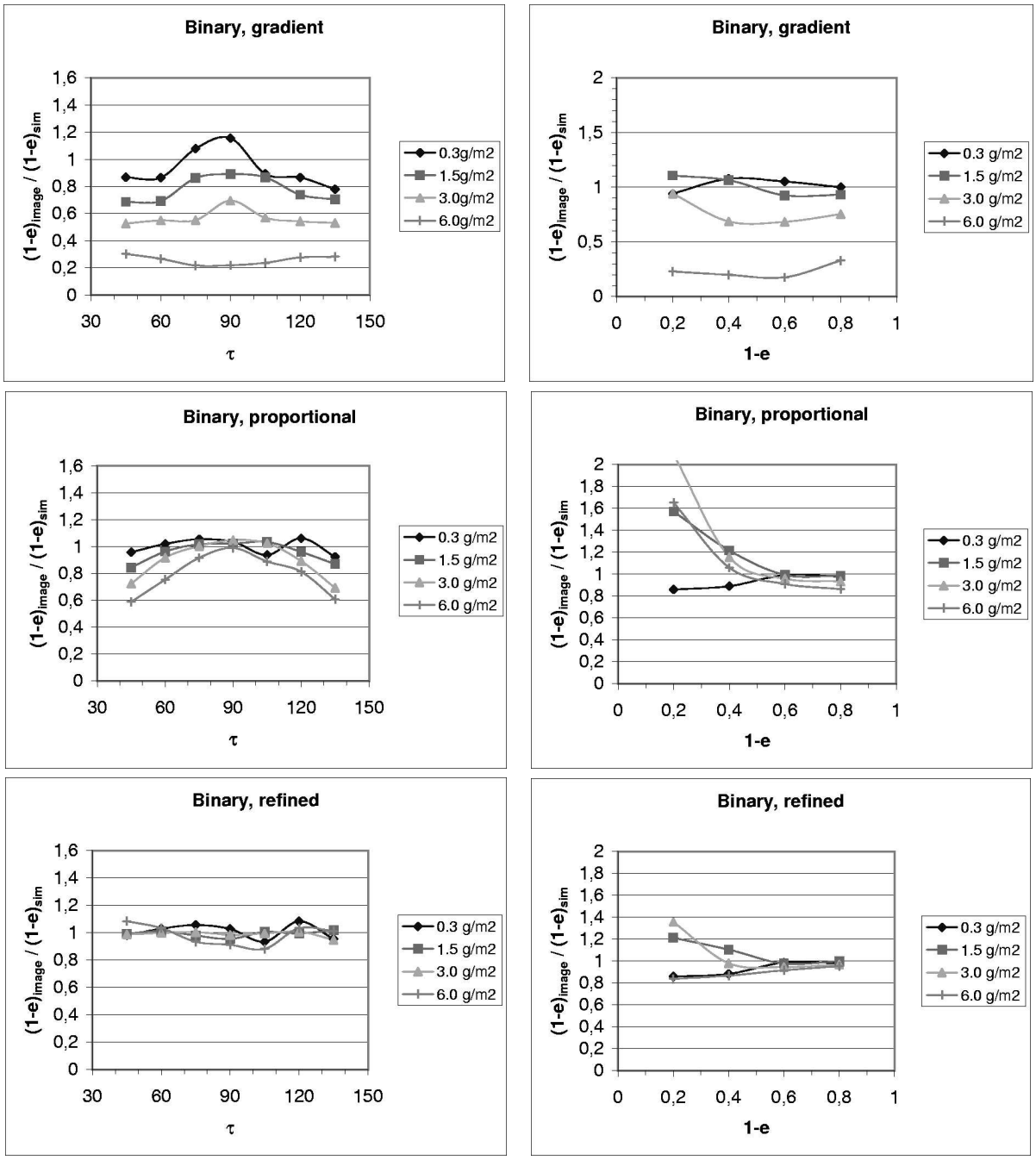

Figure 10: The determination of anisotropies in binary cases with three methods. In all cases, the grammage G varies. On the left, the true anisotropy is fixed to $1 - e = 0.5$, whereas on the right the true angle is $\tau = 90°$.

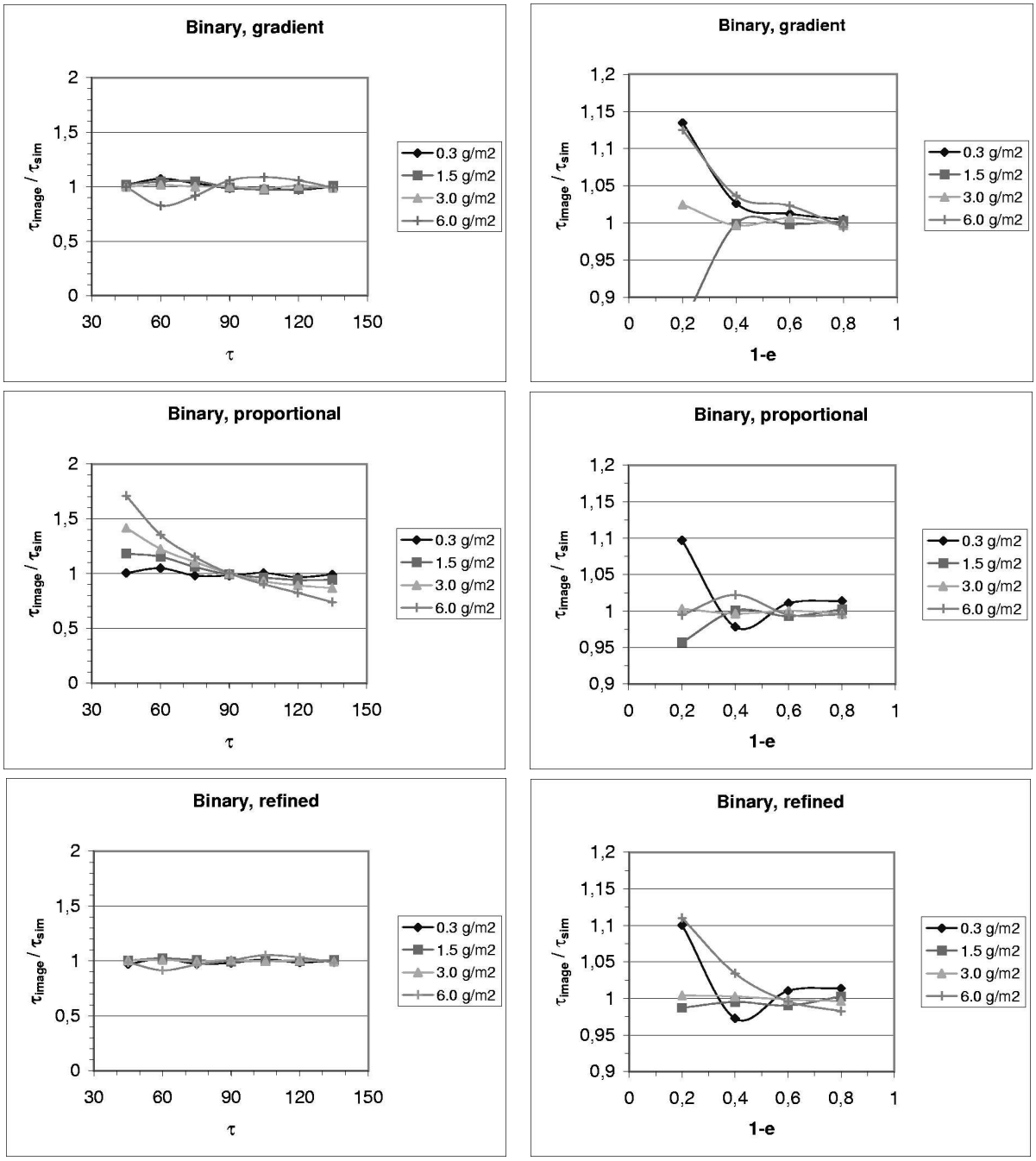

Figure 11: The determination of the angles τ in shot-noise cases with three methods. The grammage G varies in all cases. On the left, the true anisotropy is fixed to $1 - e = 0.5$, whereas on the right the true angle is $\tau = 90°$.

study area could be studied since low percentages in staining of paper fibres are advisable.

6 Acknowledgements

The authors would like to thank Technical Research Centre of Finland (VTT), and Academy of Finland for financial support.

References

Chapman, J., Kole, D., and Hellstrom, A. (2001). Papermaking with online fibre orientation measurement. *Pap. Technol.*, 42:43–46.

Cresson, T. (1988). *The Sensing, Analysis and Simulation of Paper Formation.* PhD thesis, State University of New York, Syracuse.

Erkkilä, A.-L. (1995). Paperin kerroksellisen orientaation mittaaminen ja syntymekanismit. PhL thesis, University of Jyväskylä, Jyväskylä.

Erkkilä, A.-L., Pakarinen, P., and Odell, M. (1998). Sheet forming studies using layered orientation analysis. *Pulp Paper Canad.*, 99:39–43.

Hutten, I. (1994). Paper machine evaluation by fiber orientation profile analysis. *Tappi J.*, 77:187–192.

Jeulin, D. (1989). Morphological modeling of images by sequential random functions. *Signal Proc.*, 16:403–431.

Jeulin, D. (1993). Random models for morphological analysis of powders. *J. Microsc.*, 172:13–21.

Jeulin, D. (2000). Variograms of the dead leaves model. Research Report N-31/00/MM, Paris School of Mines, Paris.

Johansson, J.-O. (2002). *Models of Surface Roughness with Application in Paper Industry.* PhD thesis, Lund University, Lund.

Kellomäki, M., Kärkkäinen, S., Penttinen, A., and Lappalainen, T. (2002). Determination of fiber orientation distribution from images of fiber networks. In *2002 Progress in Paper Physics Seminar, Finger Lakes, Syracuse, New York*, pages 102–105. SUNY-ESF, Syracuse.

Kellomäki, M., Pawlak, J. J., Sung, Y.-J., and Keller, D. S. (2001). Characterization of non-stationary structural non-uniformities in paper. In *12th Fundamental Research Symposium, Keble College, Oxford, UK*, pages 1313–1342. FRC, UK.

Kärkkäinen, S. and Jensen, E. B. V. (2001). Estimation of fibre orientation from digital images. *Image Anal. Stereol.*, 20:199–202.

Kärkkäinen, S., Jensen, E. B. V., and Jeulin, D. (2002). On the orientational analysis of planar fibre systems from digital images. *J. Microsc.*, 207:69–77.

Kärkkäinen, S., Penttinen, A., Ushakov, N. G., and Ushakova, A. P. (2001). Estimation of orientation characteristic of fibrous material. *Adv. Appl. Prob.*, 33:559–575.

Loewen, S. (1997). Fibre orientation optimization. *Pulp Paper Canad.*, 98:67–71.

Matheron, G. (1975). *Random Sets and Integral Geometry.* J. Wiley, New York.

Mecke, J. and Stoyan, D. (1980). Formulas for stationary planar fibre processes I – general theory. *Math. Operationsforsch. Statist., Ser. Statistics*, 11:267–279.

Piispanen, M. (2000). Paperiradan kuituorientaation mittaus ja säätö. *Paperi ja Puu - Paper and Timber*, 82:380–382.

Rice, J. (1977). On generalized shot noise. *Adv. Appl. Prob*, 9:553–565.

Schmidt, V. (1985). Poisson bounds for moments of shot noise processes. *Statistics*, 16:253–262.

Stoyan, D., Kendall, W. S., and Mecke, J. (1995). *Stochastic Geometry and its Applications.* J. Wiley, Chichester, 2nd edition.

Thorpe, J. (1999). Exploring fiber orientation within copy paper. In *1999 International Paper Physics Conference, San Diego, CA, USA*, pages 447–458. Tappi Press, Atlanta, GA, USA.

Xu, L., Parker, I., and Filonenko, Y. (1999). A new technique for determining fibre orientation distribution through paper. In *1999 International Paper Physics Conference, San Diego, CA, USA*, pages 421–427. Tappi Press, Atlanta, GA, USA.